

Author version: *Estuar. Coast. Shelf Sci.*, vol.94; 2011; 355-368

Rare earth elements in suspended and bottom sediments of the Mandovi estuary, central west coast of India: Influence of mining

R. Shynu*, V. Purnachandra Rao*[§], Pratima M. Kessarkar* and T. G. Rao[†]

* National Institute of Oceanography, Council of Scientific and Industrial Research (CSIR), Dona Paula, Goa – 403 004, India

[†] National Geophysical Research Institute (CSIR), Uppal Road, Hyderabad- 500 007, India

ABSTRACT

Rare earth elements (REEs) in the suspended particulate matter (SPM) of the Mandovi estuary indicated that the mean total-REEs (Σ REE) and light REE to heavy HREE ratios are lower than that of the average suspended sediment in World Rivers and Post-Archean average Australian shale. High Σ REE were associated with high SPM / low salinity and also with high SPM / high salinity. Although the Σ REE broadly agree with SPM levels at each station, their seasonal distributions along transect are different. SPM increased seaward in the estuary both during the monsoon and pre-monsoon, but consistently low at all stations during the post-monsoon. The mean Σ REE decreased marginally seaward and was < 25% at sea-end station than at river-end station. Spatial variations in Σ REE are maximum (64%) during the pre-monsoon. Strong to moderate correlation of Σ REE with Al, Fe and Mn in all seasons indicates adsorption and co-precipitation of REEs with aluminosilicate phases and Fe, Mn-oxyhydroxides. The ratio of mean Σ REE in sediment/SPM is low during the monsoon (1.27), followed by pre-monsoon (1.5) and post-monsoon (1.62). The middle REE- and heavy REE-enriched patterns with positive Ce and Eu anomalies are characteristic at every station and season, both in SPM and sediment. They also exhibit tetrad effect with distinct third and fourth tetrads. Fe-Mn ore dust is the most dominant source for REEs. However, the seasonal changes in the supply of detrital silicates, Fe-Mn ore dust and particulates resuspended from bottom sediments diluted the overall effect of salinity on fractionation and distribution of REEs in the estuary.

[§] corresponding author; e-mail: vp rao@nio.org

Keywords: rare earth elements; suspended matter, sediment, Tropical estuary, Mandovi River, western India

1. Introduction

The rare earth elements (REEs) exhibit a unique and coherent behavior during weathering, erosion and fluvial transportation due to similarity in their electronic configuration. During weathering of source rocks light REEs (LREE) are preferentially scavenged on particle surfaces, while heavy REEs (HREE) are retained in dissolved state because of stronger complexation with ligands (CO_3^{2-} , PO_4^{3-} , and organic ligands) (Byrne and Kim, 1993; Sholkovitz, 1995; Yang et al., 2002; Tang and Johannesson, 2003; Caccia and Milero, 2007). The REEs entering the river are also fractionated by the removal of certain REEs from solution due to oxy-hydroxides and (colloidal) organic matter during aqueous transport (Andersson et al., 2005; Marmolejo-Rodriguez et al., 2007). The concentrations and composition of REEs are further modified due to extensive geochemical and physico-chemical processes (coagulation, adsorption, flocculation, diagenetic remobilization and resuspension) occurring at the fresh water - seawater interface, in estuaries and in coastal systems (Sholkovitz, 1976; Hoyle et al., 1984; Ramesh et al., 1999; Censi et al., 2007; Marmolejo-Rodriguez et al., 2007). Moreover, 'monsoonal estuaries' are not in steady state. As river runoff largely spreads over only four months of the wet summer monsoon (Vijith et al., 2009) in these estuaries, identifying the sources of suspended matter in other seasons is very important. The systematic and gradual change in physico-chemical properties from La to Lu, REEs can be used (a) to characterize their provenance and (b) to better understand the processes associated with the first leg of sedimentation from river to estuary and in coastal system (Elderfield et al., 1990; Ramesh et al., 1999; Sholkovitz and Szymezak, 2000). Redistribution and fractionation of REEs between particulate and dissolved phases in estuarine waters, across a salinity gradient, and under acidic and alkaline conditions have been investigated (Elderfield and Greaves, 1982; Elbaz-Poulichet and Dupuy, 1999; Johannesson and Zhou, 1999; Borrego et al., 2005).

The Mandovi River, central west coast of India, has catchment area of $\sim 1895 \text{ km}^2$ and experiences two extreme conditions in its annual cycle. The river run off is abundant ($\sim 258 \text{ m}^3\text{s}^{-1}$, measured at the head) during the southwest monsoon (June-September) and estuarine system experiences low salinity gradient. The river run off in the remaining 8 months (October-May) is negligible ($\sim 6 \text{ m}^3\text{s}^{-1}$; Vijith et al., 2009). Due to seawater incursion the estuary system

exhibits greater salinity range during the post-monsoon (October-January) and pre-monsoon (February-May) (Shetye et al., 2007). The terrigenous flux into the estuary is visible as the surface waters look brownish, indicating abundant river-borne material, during the monsoon. Other times the waters look greenish or bluish because of plankton (Kessarkar et al., 2010) and lower river supply. Mining of Fe-Mn ores in the drainage basin upstream of the river, their transportation through the estuary by barges and uploading ores onto bigger ships in the port and offshore become an important activity during October to May. These systematic changes in hydrography of the estuary and human-induced activities affect the distribution of dissolved material and suspended / bed sediments of the estuary. A few attempts reported REE distribution in river systems (Rengarajan and Sarin, 1994; Singh and Rajamani, 2001) and in the Kavery estuary, east coast of India (Ramesh et al., 1999). Detailed studies on REEs are not made in the estuaries of western India, which characterize river-dominant flows during the monsoon and tidal current dominant flows during post- and pre-monsoons. The purpose of the present study is to report for the first time the seasonal distribution of REEs in suspended and bottom sediments of the tropical, Mandovi estuary, in order to understand their provenance and processes controlling REEs distribution and fractionation.

Previous studies in the Mandovi estuary have investigated the particulate Fe (Kamat and Sankaranarayanan, 1975) and Al (Upadhyay and Sengupta, 1995) and, trace metals in suspended and bottom sediments (Alagarsamy, 2006; Shynu et al., 2011). Kessarkar et al. (2010) and Rao et al. (2011) investigated seasonal variations in suspended matter of the Mandovi estuary along transect stations and reported estuarine turbidity maximum (ETM) as a characteristic feature, associated with high river discharge and low salinity during monsoon and, also with negligible river discharge and high salinity during pre-monsoon. The formation of ETM was attributed to the resuspension of sediments due to tidal and wind-induced currents operating in the Bay.

1.1 Geological setting

The entire territory of Goa is covered by rocks of the Goa Group belonging to the Dharwar-Super Group (Western Dharwar Craton - WDC) of the Archean-Proterozoic age, except for a narrow strip in the northeastern corner of the territory which is covered by Deccan Traps of the

Upper Cretaceous–Lower Eocene age (Gokul et al., 1985). The WDC is predominantly made up of green schist of metamorphic rocks and Tonalite-Trondhjemite Gniesses (TTG), and are characterized by high-Mg basalts and komatiites with metavolcanics and meta-sedimentary rocks (Manikyamba and Naqvi, 1997; Naqvi, 2005). The geochemistry of the Archean Trondhjemite Gniesses (Dhondial et al., 1987) and petrology and geochemistry of the mafic-ultramafic complex in Goa region (Desai et al., 2009) were investigated. The Mandovi River and its tributaries largely drain through the Bicholim formation of the Goa group in the hilly region and low-grade bauxites deposits (Al- and Fe-laterites) formed by deferrification of Precambrian rocks at the low level. The Bicholim formation is represented by quartz-chlorite-amphibole schists, metapyroclasts and tuff with calcareous, manganeseiferous and ferruginous (banded-iron formations) ore deposits (Gokul et al., 1985). The Fe-Mn ores brought from the mines are stocked along the shore of the Mandovi estuary in order to load them onto barges and transport through the estuary to the port.

2. Material and methods

Fig. 1 here

Data on REE were collected in the Mandovi estuary during June 2007–May 2008 using two approaches. (1) Surface waters were collected every alternate day at station 2, in the mid-region of the Mandovi estuarine channel, from June to September, 2007. This station is referred hereafter as the ‘regular station’ (Fig. 1). (2) Surface water, and bottom sediments were collected fortnightly at five locations, along the main channel of the Mandovi estuary (hereafter referred as ‘transect stations’), during June–September 2007, using a mechanized boat. From October 2007 to May 2008, two more stations were added at the river-end of the estuary. Five liters of each water sample were filtered through 0.4- μm Millipore filter paper. These samples were also analyzed for salinity using conductivity sensor of a portable CTD system (Seabird, SBE). The accuracy of the system for temperature and conductivity are 0.005°C and 0.0005 S/m, respectively.

2.1 Mineralogy of the SPM

Detailed mineralogy of the suspended matter from the Mandovi estuary was reported elsewhere (Kessarkar et al., 2010). The procedure for mineralogy, in brief, is as follows: The suspended sediment collected on filter paper was transferred to small beaker and made free of organic matter and carbonate by treating with H_2O_2 and acetic acid solution, respectively. They were washed with distilled water to remove the remaining acid and then concentrated the clay solution. The solution was then pipetted on glass slide and allowed them to dry in air. The sample slides were placed on a holed ceramic plate and inserted in a desiccator that contained a bowl of ethylene glycol. The desiccator was heated to 100°C for 1 hr, so that the slides were exposed to ethylene glycol vapours. Thereafter, the slides were scanned from 2° to $15^\circ 2\theta$ and from 24° to $26^\circ 2\theta$ at $1^\circ 2\theta/\text{min}$ on a Philips X-ray diffractometer, using nickel-filtered $\text{Cu K}\alpha$ radiation. Minerals were identified and their semi-quantitative abundance was calculated, following Rao and Rao (1995).

2.2 Geochemistry of the SPM

Ninety SPM samples, including 15 from the regular station and 75 from transect stations of the estuary in different months were used in major (Al, Fe and Mn) and REE determinations. The suspended matter on the filter was carefully weighed and transferred to teflon beakers. The samples were treated with $\text{HF}+\text{HNO}_3+\text{HClO}_4$ mixture in a beaker, kept overnight and then dried on a hot plate. This treatment was repeated till the sample in the beaker was completely digested. The final residue was dissolved in 20 ml of 1:1 HNO_3 . Subsequently, 5 ml of 1 ppm Rh solution was added as an internal standard and made up to the final volume (Govindaraju, 1994). These aliquots were analyzed for trace metals and REEs using a Perkin Elmer SCIEX ® (Model 6100 ELAN DRC II) Inductively-coupled plasma mass spectrometer (ICP-MS) at the National Geophysical Research Institute, Hyderabad, India. Major elements were analyzed using ICP-AES at the National Institute of Oceanography, Goa. MAG1 (Marine mud) was used as an internal standard to check the reliability of the analysis. Table 1 shows the certified values of major and rare earth elements of MAG 1 and values obtained in our experiments. The reproducibility of the results was found to be better than 5% and 10% for major and rare-earth elements, respectively.

Table 2 shows elemental concentrations of SPM on different dates at the regular station. One sample for every month was analyzed at each station for the transect stations. Table 3 shows the mean concentrations of elements at each station obtained by averaging concentration values for four months, i.e., June to September (monsoon), October to January (post-monsoon) and February to May (pre-monsoon). As we have sampled at 5 stations during monsoon and at 7 stations each during post- and pre-monsoons, the number of samples analyzed were 20 for monsoon and 28 each for post- and pre-monsoon. The mean concentrations and standard deviation are also given at each station in Table 3. Statistical treatments were carried out for the metals. The test of significance and variability of major metals and total-REEs (Σ REE) are given in Table 2 and Fig. 7.

2.3 Geochemistry of the sediment

Unlike that of SPM, bottom sediments were chosen only for 2 months in each season, i.e., June and August for monsoon, October and November for post-monsoon and February and April for pre-monsoon. A total of 38 sediments collected from transect stations of the estuary were used. The $< 2 \mu\text{m}$ fraction of the sediment was separated from the sediments using Stoke's settling velocity principle, dried and powdered. Following the aforementioned procedure, the powdered samples were digested and analyzed for major and REE concentrations. The seasonal variations of the mean concentrations at each station were calculated and given in Table 4.

3. Results

3.1. Distribution of REEs in suspended particulate matter (SPM)

3.1.1. At the Regular station (RS)

Table 2 and Fig. 2 here

Fig. 2 exhibits temporal variations of SPM concentrations, total-REEs (Σ REE), normalized ratios of light REE to heavy REE ($(L/H)_n$) and salinity (A), major clay minerals at varying SPM (B) and salinity of surface waters (C) at the regular station. The SPM, Σ REE and salinity levels during the monsoon widely ranged from 4 to 158 mg/l, 90 to 203 $\mu\text{g}\text{g}^{-1}$ and 0 to 34,

respectively. The mean Σ REE and light REEs (LREE) to heavy REEs (HREE) ratio of the SPM ($150 \mu\text{gg}^{-1}$; 20 - Table 2) indicate that the Σ REE are lower and HREE are higher than those in average suspended sediment in World Rivers (ASSWR- $174.8 \mu\text{gg}^{-1}$; 29.8) and Post-Archean average Australian shale (PAAS - $184.8 \mu\text{gg}^{-1}$; 24.7). Σ REE exhibited strong correlation with Al ($r=0.74$; $P < 0.001$) and Fe ($r=0.67$; $P < 0.01$) and moderate correlation with Mn ($r=0.55$; $P < 0.05$). Two trends can be visualized at the RS (Fig. 2A): In June, the Σ REE appear increasing with increasing SPM at salinities of 10 - 34. Mineralogy of these samples shows kaolinite, minor illite, gibbsite and goethite with traces of smectite at low SPM. But increase in smectite content from traces to 30% is found with increase in SPM concentrations (see Fig. 2B). The high SPM (158 mg/l) in July coincide with the lowest salinity, high Σ REE ($180 \mu\text{gg}^{-1}$), abundant kaolinite (55 %), followed by goethite (25 %), gibbsite (20 %) and traces of smectite (< 5%) (Figs. 2A - B). In August, Σ REE varies only $\sim 20 \mu\text{gg}^{-1}$ in 0-5 salinity range and $\sim 40 \mu\text{gg}^{-1}$ in 5–30 salinity range (Fig. 2A). The smectite content of these samples increased with increase in salinity (Fig. 2C). The PAAS-normalized REE patterns are identical despite the concentrations of SPM vary widely from 4 to 158 mg/l . They are characterized by middle REE- and heavy REE-enrichment with positive Ce (1.1) and Eu anomalies (1.4). The values of $(\text{L}/\text{H})_n$, $(\text{La}/\text{Yb})_n$ and $(\text{La}/\text{Gd})_n$ (Table 2) are low indicating that the light REEs (LREE) are lower than middle REEs (MREE) and heavy REEs (HREE). Further, the low values of $(\text{Yb}/\text{Gd})_n$ indicate that HREE are lower than MREE.

3.1.2. At transect stations

Table 3, Figs. 3-5 here

Monthly variations of SPM and Σ REE at each transect station (Fig. 3) are mostly similar with higher concentrations in monsoon and pre-monsoon seasons than in post-monsoon. Though the SPM concentrations were consistently low during the post-monsoon, Σ REE were relatively high in the early part of the post-monsoon, and then decrease gradually in the latter part. Spatial variations indicate that the concentrations of mean SPM increase from river-end to sea-end stations of the estuary, both during the monsoon and pre-monsoon, and consistently low at all stations during the post-monsoon (Fig. 4A). The Σ REE variations, however, do not exhibit this trend. The mean Σ REE at each station is the highest during the monsoon followed

by pre-monsoon and post-monsoon (Table 3). The mean $\sum\text{REE}$ decreases seaward, varies only $20 \mu\text{gg}^{-1}$ in the salinity range of 2-7 during the monsoon and $15 \mu\text{gg}^{-1}$ in the salinity range of 2.5-32 during the post-monsoon (Fig. 4A). Maximal spatial variations in $\sum\text{REE}$ ($50 \mu\text{gg}^{-1}$) occurred during the pre-monsoon in the salinity range of 10-34, with relatively high values at the river-end stations and nearly identical values at sea-end stations (Fig. 4A). Marginal decrease in $(\text{L}/\text{H})_n$ values with increase in salinity towards sea-end stations is characteristic in all seasons (Fig. 4A). The PAAS-normalized REE patterns are similar and are characterized by MREE- and HREE-enrichment with positive Ce and Eu anomalies (Fig. 4B; Table 3). They are partitioned into four segments, La-Nd, Pm-Gd, Gd-Ho and Er-Lu, called tetrads (Censi et al., 2007). Four Tetrads were convex and are typical in pattern (Fig. 4B). The third and fourth tetrads were more distinctive than that of one and two, which are affected by strong positive Ce and Eu anomalies. The mean Al, Fe and Mn values and Ce and Eu anomalies, in general, decrease seaward, except that the Fe and Eu anomaly increase seaward during the post-monsoon (Fig. 5A-F). The ratios of $(\text{La}/\text{Yb})_n$ and $(\text{La}/\text{Gd})_n$ also decreased seaward, but the ratios of $(\text{Yb}/\text{Gd})_n$ increased marginally seaward in all seasons (Fig. 5G-I). Kessarkar et al. (2010) reported kaolinite, gibbsite, goethite and illite with traces of smectite at river-end stations, and increasing smectite concentrations with proportional decrease in other clay minerals towards sea-end stations, both during monsoon and pre-monsoon. Kaolinite and traces of other clay minerals occur at all stations during the post-monsoon.

3.2. Distribution of REEs in bottom sediments

Table 4 and Fig.6 here

The mean $\sum\text{REE}$ of bottom sediments (Table 4) is the highest during the monsoon ($196.6 \mu\text{gg}^{-1}$), followed by near equal values in pre- monsoon ($184.4 \mu\text{gg}^{-1}$) and post-monsoon ($182.1 \mu\text{gg}^{-1}$). The ratios of mean $\sum\text{REE}$ in sediment to that in SPM are 1.27, 1.62 and 1.5 for the monsoon, post-monsoon and pre-monsoon, respectively. The $\sum\text{REE}$ of sediment exhibited relatively high values at river-end and sea-end stations, with lower values in between during monsoon and relatively high values at mid-stations (4 and 5) during post-monsoon (Fig. 6A). The $\sum\text{REE}$ of sediment at sea-end stations (1-3) is higher than that of river-end stations (5-7) during the pre-monsoon. The seaward decrease in $(\text{L}/\text{H})_n$ and $(\text{La}/\text{Yb})_n$ indicates increase in

HREE (Table 4). The PAAS-normalized REE patterns of sediment are typical to that of SPM and are characterized by MREE- and HREE-enriched patterns, with distinct positive Ce and Eu anomalies (Table 4). Tetrad effect is also seen in all sediment samples (Fig. 6B).

3.3. Relationship of Σ REE with Al, Fe and Mn

Fig. 7 here

The mean concentrations of Al, Fe and Mn and their spatial distribution varied seasonally (Tables 3 and 4). The Fe/Al and Mn/Al ratios of SPM decrease from station 7 at the river-end to station 1 at sea-end of the estuary in all seasons. The mean Fe/Al and Mn/Al ratios are lower (1.37 and 0.08) during the monsoon but distinctly higher during the post- (1.86 and 0.16) and pre-monsoons (1.55 and 0.16). The Al and Fe show significant ($P < 0.001$) to moderate ($P < 0.05$) correlation with Σ REE in all seasons, whereas Mn shows strong correlation with Σ REE during monsoon and weak correlation ($P < 0.1$) during the post- and pre-monsoons (see Fig. 7). On the other hand, the mean concentrations of Al and Fe in bottom sediments do not show sharp decrease towards sea-end stations in all the seasons, while Mn showed sharp decrease (Table 4). The mean Fe/Al ratio of sediments (1.38) is same as that in SPM (1.37) during monsoon, but lower (1.1 to 1.2) than in SPM (1.55 to 1.86) during the post- and pre-monsoons. The mean Mn/Al ratio of sediment is higher (0.13) than in SPM (0.08) during monsoon, but lower (0.07) than in SPM (0.16) during post- and pre-monsoons. The Σ REE of sediment yielded strong correlation with Fe ($r=0.76$ to 0.71 ; $P < 0.01$) during monsoon and post-monsoon and, non-significant relation during pre-monsoon (Fig. 7). Σ REE of sediment showed moderate correlation with Mn ($r=0.5$ to 0.64 ; $P < 0.05$) and non-significant relation with Al in all seasons.

4. Discussions

4.1 Controls on Σ REE of SPM at the regular station (RS)

Temporal variations in Σ REE at the regular station (Fig. 2) are affected by changes in both salinity and SPM during the monsoon. Suspended matter with abundant kaolinite together with gibbsite indicates intense chemical weathering of the hinterland rocks. Goethite, a colloidal iron-oxyhydroxide is also an important component in SPM. Occurrence of the highest Σ REE along with the highest SPM (consisting of abundant kaolinite, gibbsite and goethite) and the

lowest salinity during the peak monsoon (July; Fig. 2A-B) indicates that REEs are transported mainly by river run off. River waters contain colloidal materials. Large scale removal of REEs occurs in the estuarine environment by co-precipitation and adsorbing onto Fe-O-OH surfaces (Elderfield et al., 1990; Andersson et al., 2005; Marmolejo-Rodríguez et al., 2007). The Fe-Mn ore deposits stored along the shores of the estuary also serve as source for dissolved and particulate Fe- and Mn-oxyhydroxides that are drained into the estuary during heavy monsoon rains. Strong to moderate correlations of Σ REE with Al, Fe and Mn indicate that clay minerals and Fe-Mn-oxyhydroxides are important carriers of REEs. Taylor and McLennan (1985) suggested that the REEs are enriched in fine-grained sediments, especially clay minerals.

The Σ REE values are relatively high at low salinities (<10 - see July and August) as well as at high salinities (~30; June in Fig. 2A). High SPM associated with high salinity (see June–Fig. 2A) at regular station was attributed to the development of estuarine turbidity maximum (ETM; Kessarkar et al., 2010). Therefore, Σ REE may have been affected by two sources: (a) Σ REE associated with low salinities implies supplies from river discharges along with detrital matter, and (b) Σ REE with intermediate or high salinities, i.e., processes (resuspension, flocculation and coagulation) associated with the ETM. Mixing of sediments between the two sources in different proportions driven by water circulation resulted in the observed temporal variations in the abundance of Σ REE.

The gradual increase in smectite coincided with increase in SPM (Fig. 2B) and salinity (Fig. 2C) but with marginal decrease in $(\text{LREE}/\text{HREE})_n$ (i.e., increase in HREEs). This suggests that smectite may have been resuspended from the bottom as the turbidity reached maximum value. The grain size of smectite is smaller than that of kaolinite and illite. Smectite particles have relatively large surface area and greater negative charge and thus form stronger complexes with organic compounds than other clay minerals (Degens and Ittekkot, 1984). Heavy REEs form stronger complexes with ligands in solution of high ionic strength (Coppin et al., 2002) and also with finer particles. The association of high heavy REEs and smectites at high salinity thus indicates stronger association between the two. Finer particles flocculate through aggregation in ETM and thus HREE are preferentially removed during flocculation.

Identical shale-normalized REE patterns despite changing SPM concentrations at the regular station indicate REEs have not been fractionated during resuspension.

4.2 Controls on Σ REE of SPM at transect stations

4.2.1 Monsoon

General agreement between Σ REE and SPM at each station (Fig. 3) indicates the control of suspended matter on Σ REE distribution. Distinct spatial differences in the distribution of SPM and Σ REE (Fig. 4A), however, suggest involvement of other factors. The mean salinity during the monsoon ranged between 2 and 7 (Fig. 4A). Increase in salinity facilitates coagulation and flocculation, and hence removal of REEs (dissolved and suspended matter associated) from the water column. Sholkovitz (1993) indicated that 60-90% of the river input REEs are removed in estuaries. Hoyle et al. (1984) and Sholkovitz (1993) suggested that the large scale removal of REEs (>70% complete by salinity 5) is associated with Fe-organic colloids and their flocculation during the early estuarine mixing. The decrease in Σ REEs is only marginal (< 25%) at sea-end station (Fig. 4A). Spatial variations in ratios of $(La/Yb)_n$, $(La/Gd)_n$ and $(Yb/Gd)_n$ (Fig. 5G) are also small during the monsoon. On the other hand, the increase in SPM concentrations towards sea-end stations (Fig. 4A) has been attributed to the prevalence of estuarine turbidity maximum (Kessarkar et al., 2010), due to which particulate matter is supplied to the water column through resuspension of bottom sediments. It appears that Σ REE are affected by two opposing processes: the low salinity effect that tends to remove Σ REEs from suspension is countered by ETM when REEs resuspended back into the water column. The combined influence of these processes minimized the differences in Σ REE between river-end and sea-end stations. Elderfield et al. (1990) showed REE maximum in the Delaware River estuary is associated with significant turbidity maximum zone, reflecting the processes in ETM. Minor spatial variations in $(La/Yb)_n$, $(La/Gd)_n$ and $(Yb/Gd)_n$ (Fig. 5G) indicate dilution of river-borne REEs with resuspended material from bottom sediment at sea-end stations.

4.2.2 Post-monsoon

The least SPM concentrations at all stations, low or lowest mean ΣREE during the post-monsoon (Figs. 3 and 4) and sharp decrease in the mean Al from monsoon to post-monsoon (Table 3) indicate negligible terrigenous supply through river run off. Although one would expect removal of REEs and Fe in the estuary (Elderfield et al., 1990), across a salinity gradient of 2.5 to 32, ΣREE changed only by $15 \mu\text{gg}^{-1}$ between river-end and sea-end stations (Fig. 4A) while the mean Fe increase seaward (Fig. 5B). This meager removal of ΣREE and increases in Fe and Al (stations 2, 3 and 4 in Fig. 5B) point to additional sources in the estuary, either due to inputs from the Cumbarjua canal (joining the estuary at stations 4 and 5—see Fig. 1) or to the spillage of Fe-Mn ores during transportation. Higher Fe and Al values and ΣREE at stations 4 and 5 (Table 3; Figs. 4A and 5B) attest the influence of canal. High Fe/Al and Mn/Al ratios during post-monsoon suggest additional source of Fe and Mn, other than detrital. Strong correlation of ΣREE with Fe (Fig. 7) is an evidence for association of REEs with Fe-rich colloids. The pulverized Fe-Mn ore materials, loaded onto barges at different points along the estuary from October, are transported through the estuary and uploaded onto bigger ships in the offshore waters. Therefore, spill over of pulverized Fe - Mn ore dust into the estuary is likely to have been responsible for the observed REEs. Thus the Fe-Mn dust from ore deposits and minor detrital supply at mid-stations diluted the overall effect of salinity on ΣREE and facilitated to maintain least difference in ΣREE between river-end and sea-end stations.

4.2.3 Pre-monsoon

The seaward increase in SPM concentrations during the pre-monsoon (Fig. 4A) was attributed to the tidal and wind-driven turbidity maximum (Kessarkar et al., 2010). Similar reasoning may be applicable for the increase in mean ΣREE ($126 \mu\text{gg}^{-1}$) at the sea-end stations (1-3) of the estuary during the pre-monsoon (Fig. 3-4A; Table 3) compared to that in post-monsoon ($105 \mu\text{gg}^{-1}$). It is supported by the decrease in the mean Fe/Al ratio from post-monsoon (1.86) to pre-monsoon (1.55) indicating increased Al concentrations may be due to resuspension by turbidity. Upadhyay and Sengupta (1995) also reported increase in dissolved Al with increase in salinity during the pre-monsoon and attributed it to resuspension. Continuous resuspension

of sediment in the zone of turbidity maximum, and spill over of Fe-Mn ores from the barges are probably responsible for maintaining near equal concentrations of Σ REEs at sea-end stations.

4.3 Controls on Σ REE in sediments

The ratios of mean Σ REE of sediment/SPM simply reflect contributions from different sources. As indicated earlier, the sources of Σ REE to the water column are detrital silicates, Fe, Mn-oxyhydroxides and resuspended material from bottom sediment during the monsoon, largely Fe-Mn ore dust during the post-monsoon, and Fe-Mn ore dust and resuspended material during the pre-monsoon. Accordingly, the concentrations of REEs settled from water column to the sediment varied. Strong correlation of Σ REE with Fe ($P < 0.001$), moderate correlation with Mn ($P < 0.05$) and weak or no correlation with Al in sediments (Fig. 7) suggest that REEs associated with detrital clay particles deposited at the bottom were suspended frequently because of intense turbidity. As a consequence, REEs associated with Fe, Mn-oxyhydroxide particulates are concentrated and retained in sediments. The mean Mn/Al ratios in SPM and sediment are 0.08 and 0.13 during monsoon, 0.16 and 0.07 during post-monsoon and 0.16 and 0.05 during pre-monsoon. The increase in Mn/Al ratio in SPM and its proportional decrease in sediments from monsoon to post-monsoon and to pre-monsoon (Tables 3 and 4) suggest that some diagenetic Mn released from sediments may have been precipitated/adsorbed in the water column. This is in addition to Mn from Fe-Mn ore dust spilled over during transportation. Higher concentrations of Fe in SPM during post- and pre-monsoons (Fig. 5) may indicate spillover from ore dust during transportation through estuary, unloading activities at the port and some diagenetic Fe recycled into the water column.

4.4 Fractionation of REEs and Eu and Ce anomalies

The LREE/HREE ratio is usually controlled by the geology of the drainage basin and/or concentrations of heavy minerals. The river-borne SPM is transported into the estuary only during the monsoon. The normalized mean ratios of La/Yb and La/Gd (Fig. 5G-I; Table 2-4) indicate that LREE are lower than MREE and HREE in all seasons. Moreover, positive Eu and Ce anomalies and MREE- and HREE-enriched patterns are invariably present in SPM and sediment (Figs. 4B and 6B). Several workers reported MREE-enriched patterns in colloidal

Mn- and Fe-oxyhydroxides (Palmer and Elderfield, 1986; Bau, 1999; Ohta and Kawabe, 2001 and Quinn et al., 2006) and colloidal organic matter (Tang and Johannesson, 2010). Therefore the sources other than heavy minerals, most probably Fe, Mn-ore material and to a certain extent detrital and organic input contributed REEs to the estuarine system.

Positive Eu anomaly is a characteristic of shale-normalized REE patterns (Figs. 4B and 6B). Positive Eu anomalies are usually associated with aeolian input, basic volcanic materials, hydrothermal fluids or anthropogenic organic pollutants (Michard et al., 1983; Ruhlman and Owen, 1986; Oudin and Cocherie, 1988; Elderfield, 1988; Nozaki et al., 2000; Tang and Johannesson, 2003). Allen et al. (1985) showed positive Eu anomaly for the charnokites of southern India. The Mandovi River drains through schists, gneisses and banded-iron formations and manganeseiferous deposits (see Section 1.1) in the upstream and low-grade bauxite and lateritic formations in the downstream (Desai et al., 2009). Fractionated REE patterns with positive Eu anomaly are characteristic of banded-iron formations, Tonalite-Trondhjemite Gneisses (TTG) and Fe-Mn bearing arenites (Srinivasan et al., 1989; Manikyamba and Naqvi, 1997; Naqvi, 2005). They suggested that their FeO, SiO₂ and REEs are provided by primary hydrothermal fluids emplaced at vent sites of Archean oceanic ridges. The shale-normalized REE patterns of the Trondhjemite Gneisses (Dhondial et al., 1987) and mafic-ultramafic complex from Goa (Desai et al., 2009), and Fe-Mn ores from Goa (Fig. 4B) indeed show positive Eu anomaly and HREE-enriched patterns. Eu anomaly increases with increase in Fe in the post-monsoon (see Figs. 5B and 5E), during which Fe, Mn ores are major contributors of particulate matter into the estuary. We therefore suggest that the Eu anomaly is probably inherited from hinterland rocks and Fe-Mn ores, and their weathered products continued to carry this signature in SPM and in sediment.

Positive Ce anomaly is also present both in SPM and sediment (Figs. 4B, 5D-F and 6B). As Ce anomaly also occurs in Fe-Mn ores (Fig. 4B) it may be because of Ce oxidation at Mn- and Fe-oxyhydroxide surface (De Carlo et al., 1998; Bau, 1999; Ohta and Kawabe, 2001) and thus inherited from hinterland rocks. Sholkovitz (1993), Nozaki et al. (2000) and Horbe and da Costa (2005) showed the presence of Ce anomaly in the tropical rivers mainly due to the

scavenging of Ce in oxides, principally iron oxyhydroxides. Strong Ce removal is associated with coagulation of river colloids and biological productivity and as a consequence positive Ce anomaly is expected in the fluvial components of the inshore sediments. Tachikawa et al. (1997) have shown that the positive Ce anomaly in SPM was developed by adsorption of REE (III) onto the particulate MnO_2 surfaces. The positive Ce anomalies may have been caused by high stability of Ce in river water facilitated by the abundant occurrence of Fe-Mn ore materials.

The tetrad effect, a split of REE patterns into four convex-shaped segments, is a characteristic feature of SPM (Fig. 4B) and sediment (Fig. 6B). Bau (1996) suggested that it is caused by complexation of REEs, when adsorption, co-precipitation, dissolution, and/or ligand-exchange reactions occur. Censi et al. (2007) reported MREE-enriched REE patterns with negative Eu anomaly and lanthanide tetrad effects in the dissolved phase and SPM of the estuary in Thailand's Mae Klong River and offered similar explanation by Bau (1996) for the tetrad effect. Besides tetrads, positive Ce and Eu anomalies and high HREEs are also present in our REE-patterns when compared to that of Censi et al. (2007). As discussed above, Eu anomaly is caused by the emplacement of hydrothermal fluids at the vent sites of Archean oceanic ridges. Eu anomaly and HREEs are dominant in Fe-Mn ore of Goa (see Fig. 4B). On the other hand, Monecke et al. (2002, 2006) and Broska et al. (2006) reported lanthanide tetrad effect in highly evolved granitic rock systems as an indicator of the transition between magmatic to high-temperature hydrothermal system and suggested that the tetrad effect can not be modeled as fractional crystallization, indicated by Bau (1996) and Irber (1999). The formation of convex tetrads is the result of complexation of REEs in hydrothermal system, introduced during hydrothermal fluid-rock interactions and before emplacement in the sub-volcanic environment where phase separation caused a split of the system into fluid and magma subsystems. Since the material contributed by Fe-Mn ores is a predominant component annually and, Eu anomaly and tetrad effect are typical for both SPM and sediment (Figs. 4B and 6B) we suggest that the tetrads are mostly inherited from hinterland rocks, introduced during hydrothermal fluid-rock interactions during or after emplacement of magma.

The seaward increase in HREEs is evident from the decrease in $(L/H)_n$ and $(La/Yb)_n$ and increase in $(Yb/Gd)_n$ (Figs. 4A, 5G-I). HREEs are usually associated with fine-grained particles. The increase in $(Yb/Gd)_n$ is associated with the increase in Fe and Eu anomaly during the post-monsoon and Eu anomaly during the pre-monsoon (Figs. 5B, 5E-F, 5H-I). As high Fe and HREEs and, Eu anomaly are characteristic of Fe-Mn ores (Fig. 4B) we suggest that the fine-grained, Fe-Mn ore particulates, that spilled over during transport through the estuary and unloading operations in the port region, contributed abundantly to the distribution of REEs in the estuary.

Acknowledgements

We thank the Director, National Institute of Oceanography, Goa for his keen interest on 'Mandovi Monsoon Experiment' and facilities. Funds for the Project Assistant are from the Project 'SIP 1308'. Fellowship for R. Shynu and expenditure for carrying out analyses was supported by Project funds from the Ministry of Earth Sciences (GAP 2002) and Department of Science and Technology, New Delhi (GAP 2196). We sincerely thank Dr. M. Dileepkumar, two anonymous reviewers and editor, ECSS for their critical comments and suggestions on our earlier manuscript. This is NIO contribution---

References

- Alagarsamy, R., 2006. Distribution and seasonal variation of trace metals in surface sediments of the Mandovi estuary, west coast of India. *Estuarine Coastal and Shelf Science* 67, 333-339.
- Allen, P., Condie, K.C., Narayana, B.L., 1985. Geochemistry of prograde and retrograde charnockite-gneiss reactions in southern India. *Geochimica et Cosmochimica Acta* 49, 323-336.
- Andersson, K., Dahlqvist, R., Turner, D., Stolpe, B., Larsson, T., Ingri, J., Andersson, P., 2005. Colloidal rare earth elements in a boreal river: Changing sources and distributions during the spring flood. *Geochimica et Cosmochimica Acta* 70, 3261-3274.
- Bau, M., 1996. Controls on the fractionation of isovalent trace elements in magmatic and aqueous systems: evidence from Y/Ho, Zr/Hf, and lanthanide tetrad effect, *Contributions to Mineralogy and Petrology* 123, 323-333.

- Bau, M., 1999. Scavenging of yttrium and rare earths by precipitating iron oxyhydroxide: experimental evidence for Ce oxidation, Y-Ho fractionation and lanthanide tetrad effect. *Geochimica et Cosmochimica Acta* 63, 67-77.
- Byrne, R., Kim, K., 1993. Rare earth precipitation and coprecipitation behaviour: The limiting role of PO_4^{3-} ion dissolved REE concentrations in seawater. *Geochimica et Cosmochimica Acta* 57, 519-526.
- Borrego, J., Lo'pez-Gonza'lez, N., Carro, B., Lozano-Soria, O., 2005. Geochemistry of rare-earth elements in Holocene sediments of an acidic estuary: Environmental markers (Tinto River Estuary, South-Western Spain). *Journal of Geochemical Exploration* 86, 119– 129.
- Broska, L., Gaab, A., Kubis, M., 2006. Tetrad effect in the western Carpathians granites and their petrological interpretation. *Acta Mineralogica-Petrographia, Abstract Series* 5, Szeged, 19.
- Caccia, V.G., Milero, J.F., 2007. Distribution of yttrium and rare earths in Florida Bay sediments. *Marine Chemistry* 104, 171–185
- Censi, P., Sprovieri, M., Saiano, F., Di Geronimo, S.I., Larocca, D., Placenti, F., 2007. The behaviour of REEs in Thailand's Mae Klong estuary: Suggestions from the Y/Ho ratios and lanthanide tetrad effects. *Estuarine, Coastal and Shelf Science* 71, 569-579.
- Coppin, F., Berger, G., Bauer, A., Caslet, S., Loubet, M., 2002. Sorption of lanthanides on smectite and kaolinite. *Chemical Geology* 182, 57-68.
- De Carlo, E., Wen, X.Y., Irving, M. 1998. The influence of redox reactions on the uptake of dissolved Ce by suspended Fe and Mn oxide particles. *Aquatic Geochemistry* 3, 357-389.
- Degens, E.T., Ittekkot, V., 1984. A new look at clay-organic interactions, In Nord-Sud profil, Zentraleuropa-Mittelmeerraum Afrika, *Mitteilungen aus dem Geologisch-Paleontologischen*, ed. F. G. Knetsch, Institute der Universitat Hamburg. Heft 56, 229-248.
- Desai, A.G., Arolkar, D.B., French, D., Viegas, A., Vishwanath, T.A., 2009. Petrogenesis of the Bondla layered mafic-ultramafic complex Usgaon, Goa. *Journal of Geological Society of India* 73, 697-714.
- Dhondial, D.P., Paul, D.K., Sarkar, A., Trivedi, J.R., Gopalan, K., Potts, P.J., 1987. Geochronology and geochemistry of the Precambrian granitic rocks of Goa, SW India. *Precambrian Research* 36, 287-302.
- Elbaz-Poulichet, F., Dupuy, C., 1999. Behaviour of rare earth elements at the freshwater–seawater interface of two acid mine rivers: the Tinto and Odiel (Andalucia, Spain). *Applied Geochemistry* 14, 1063–1072.

- Elderfield, H., Greaves, M.J., 1982. The rare-earth elements in seawater. *Nature* 296, 214-219.
- Elderfield, H. 1988. The oceanic chemistry of the rare-earth elements. *Philosophical Transactions of Royal Society London A* 325, 105–126.
- Elderfield, H., Upstill-Goodard, R., Sholkovitz, E.R., 1990. The rare earth elements in rivers, estuaries and coastal seas and their significance to the composition of seawater. *Geochimica et Cosmochimica Acta* 54, 971-991.
- Gokul, A.R., Srinivasan, M.D., Gopalakrishnan, K., Viswanathan, L.S., 1985. Stratigraphy and Structure of Goa. Seminar Volume on Earth Resources for Goa's Development, Geological Survey of India, 1–13.
- Govindaraju K. 1994. Compilation of working values and sample description for 383 Geostandards. *Geostandard Newsletter*, 18 (Special issue) 158 pp.
- Horbe, A.M.C., da Costa, M.L., 2005. Lateritic crusts and related soil in eastern Brazilian Amazonia. *Geoderma* 126, 225–239
- Hoyle, J., Elderfield, H., Gledhill, A., Greaves, M., 1984. The behaviour of rare earth elements during mixing of river and sea waters. *Geochimica et Cosmochimica Acta* 48, 143- 149..
- Irber, W., 1999. The lanthanide tetrad effect and its correlation with K/Rb, Eu/Eu*, Sr/Eu, Y/Ho, and Zr/Hf of evolving per aluminous granite suites. *Geochimica et Cosmochimica Acta* 63, 489–508.
- Johannesson, K.H., Zhou, X., 1999. Origin of middle rare earth elements enrichments in acid waters of a Canadian High Arctic lake. *Geochimica et Cosmochimica Acta* 61, 153–165.
- Kamat, S.B., Sankaranarayanan, V. N., 1975. Concentration of particulate iron in estuarine and coastal waters of Goa. *Indian Journal of Marine Sciences* 4, 34-38.
- Kessarkar, P.M., Rao, V.P., Shynu, R., 2010. The nature and distribution of particulate matter in the Mandovi estuary, central west coast of India, *Estuaries and Coasts* 33, 30-44.
- Manikyamba, C., Naqvi, S.M., 1997. Mineralogy and geochemistry of Archaean greenstone belt-hosted Mn formations and deposits of the Dharwar Craton: redox potential of proto-oceans. In: Nicholson, K., Hein, J.R., Buhn, B. and Dasgupta, S. (Eds.), *Manganese mineralization: geochemistry and mineralogy of Terrestrial and Marine deposits*, Geological Society Special Publication 119, pp. 91-103.
- Marmolejo-Rodríguez, A.J., Prego, R., Meyer-Willerer, A., Shumilin, E., Sapozhnikov, D., 2007. Rare earth elements in iron oxy-hydroxide rich sediments from the Marabasco

River-Estuary System (Pacific coast of Mexico), REE affinity with iron and aluminium. *Journal of Geochemical Exploration* 94, 43-51.

McLennan, S.M., 1989. Rare earth elements in sedimentary rocks: influence of provenance and sedimentary processes. In: Lipin B.R and G.A. McKay (editors), *Geochemistry and mineralogy of rare earth elements*. *Reviews in Mineralogy* 21, 169-200.

Michard, A., Albarede, F., Michard, G., Minster, J.F., Charlou, J.L., 1983. Rare-earth elements and uranium in high-temperature solutions from East Pacific Rise hydrothermal vent field (13° N). *Nature* 303, 795-787.

Monecke, T., Dulsi, P., Kempe, U., 2006. Origin of convex tetrads in rare earth element pattern of hydrothermally altered siliceous igneous rocks from the Zinnwald Sn W deposit, Germany. *Geochemica et Cosmochemica Acta* 71, 335-353.

Monecke, T., Kempe, U., Monecke, J., Sala, M., Wolf, D., 2002. Tetrad effect in rare earth element distribution patterns: A method of quantification with application to rock and mineral samples from granite-related rare metal deposits. *Geochimica et Cosmochimica Acta* 66, 1185–1196.

Naqvi, S.M., 2005. *Geology and evolution of the Indian Plate (from Hadean to Holocene (4 Ga to 4 Ka))*, Capital publishing company, New Delhi, 450p.

Nozaki, Y., Lerche, D., Sotto, A.D., Snidvongs, A., 2000. The estuarine geochemistry of rare earth elements and Indium in the Chao Phraya River, Thailand. *Geochimica et Cosmochimica Acta* 64, 2983–3994.

Ohta, A., Kawabe, I., 2001. REE (III) adsorption onto Mn dioxide and oxyhydroxide: Ce(III) oxidation by delta MnO₂. *Geochimica et Cosmochimica Acta* 65, 695-703.

Palmer, M.R., Elderfield, H., 1986. Rare earth elements and neodymium isotopes in ferromanganese oxide coatings on Cenozoic foraminifera from the Atlantic Ocean. *Geochimica et Cosmochimica Acta* 50, 409-417.

Oudin, E., Cocherie, A., 1988. Fish debris record the hydrothermal activity in the Atlantis II Deep sediments (Red Sea). *Geochimica et Cosmochimica Acta* 52, 177–184.

Quinn, K.A., Byrne, R.H., Scijf, J. 2006. Sorption of yttrium and rare earth elements by amorphous ferric-hydroxide: influence of solution complexation with carbonate. *Geochimica et Cosmochimica Acta* 70, 4151-4165.

Ramesh, R., Ramanathan, A.L., Arthur James, R., Subramanian, V., Jacobsen, S.B. and Holland, H.D. 1999. Rare earth elements and heavy metal distribution in estuarine sediments of east coast of India. *Hydrobiologia* 57, 1–11.

- Rao, V.P., Shynu, R., Kessarkar, P.M., Sundar, D., Michael, G.S., Narvekar, T., Blossom, V., Mehra, P., 2011. Suspended sediment dynamics on a seasonal scale in the Mandovi and Zuari estuaries, Central west coast of India. *Estuarine, Coastal and Shelf Science* 91, 78-86.
- Rao, V.P., Rao, B.R., 1995. Provenance and distribution of clay minerals in the continental shelf and slope sediments of the west coast of India. *Continental Shelf Research* 15, 1757-1771.
- Rengerajan, R., Sarin, M.M., 1994. Distribution of rare earth elements in the Yamuna and the Chambal rivers, India. *Geochemical Journal* 38, 551-569.
- Rollinson, H., 1993. Using trace elements data. *In*. Rollinson, H., (editor), *Using geochemical data: evaluation, presentation, interpretation*. Pearson, Prentice Hall, pp. 133-134.
- Ruhlin, D.E., Owen, R.M., 1986. The rare earth element geochemistry of hydrothermal sediments from the East Pacific Rise: Examination of a sea-water scavenging mechanism. *Geochimica et Cosmochimica Acta* 50, 393-400.
- Shetye, S.R., Kumar, M.D., Shankar, D., 2007. *The Mandovi and Zuari estuaries*. National Institute of Oceanography, Goa. 145 p.
- Sholkovitz, E.R., 1976. Flocculation of dissolved organic and inorganic matter during the mixing of river water and seawater. *Geochimica et Cosmochimica Acta* 40, 831-845.
- Sholkovitz, E.R., 1993. The geochemistry of rare earth elements in the Amazon River estuary. *Geochimica et Cosmochimica Acta* 57, 2181-2190.
- Sholkovitz, E.R., 1995. The aquatic chemistry of rare earth elements in rivers and estuaries. *Aquatic Geochemistry* 1, 1-34.
- Sholkovitz, E., Szymezak, R., 2000. The estuarine chemistry of rare earth elements: comparison of the Amazon, Fly, Sepik and Gulf of Papua systems. *Earth and Planetary Science Letters* 178, 299-309.
- Singh, P., Rajamani, V., 2001. Geochemistry of the floodplain sediments of the Kaveri river, Southern India. *Journal of Sedimentary Research* 71, 50-60.
- Srinivasan, R., Naqvi, S.M., Uday Raj, B., Subbarao, D.V., Balaram, V., Rao, T.G., 1989. Geochemistry of the Archaean greywackes from the northwestern part of Chitradurga Schist Belt, Dharwar Craton, South India- evidence for granetoid upper crust in the Archaean. *Journal of Geological Society of India* 34, 505-516.

- Tachikawa, K., Jeandel, C., Roy-Barman, M., 1997. A new approach to the Nd residence time in the ocean: the role of atmospheric inputs. *Earth and Planetary Science Letters* 170, 433– 446.
- Tang, J., Johannesson, K.H., 2003. Speciation of rare earth elements in natural terrestrial waters: assessing the role of dissolved organic matter from the modeling approach. *Geochimica et Cosmochimica Acta* 67, 2321– 2339.
- Tang, J., Johannesson, K.H., 2010. Ligand extraction of rare earth elements from aquifer sediments: implications for rare earth element complexation with organic matter in natural waters. *Geochimica et Cosmochimica Acta*, doi:10.1016/j.gca.2010.08.028
- Taylor, S.R., McLennan, S.M., 1985. *The Continental Crust: Its Composition and Evolution*. Blackwell, Oxford, 312.
- Upadhyay, S., Sengupta, R., 1995. The behavior of aluminium in waters of the Mandovi estuary, west coast of India. *Marine Chemistry* 51, 261-276.
- Viers, J., Dupre, B., Gaillardet, J., 2009. Chemical composition of suspended sediments in World Rivers: New insights from a new database. *Science and Total Environment* 407, 853-868.
- Vijith, V., Sundar, D., Shetye, S. R., 2009. Time-dependence of salinity in monsoonal estuaries. *Estuarine, Coastal and Shelf Science* 85, 601-608.
- Yang, S.Y., Jung, H.S., Choi, M.S., Li, C.X., 2002. The rare earth element compositions of the Changjiang (Yangtze) and Huanghe (Yellow) river sediments. *Earth and Planetary Science Letters* 201, 407– 419.

Figure Captions

Fig. 1. Station locations in the Mandovi estuary, Goa, Central west coast of India.

Fig. 2. (A) Variations in Σ REEs, suspended particulate matter (SPM), salinity and normalized ratio of LREE/HREE $(L/H)_n$ in suspended matter at the regular station (RS, station 2). (B) X-ray diffractograms of SPM arranged with increasing concentrations of SPM in June / July, and (C) of salinity in August. Minerals are shown as: S- smectite, I- illite, K- kaolinite, Gi-gibbsite, Go-goethite. S followed by number in bracket in Fig. 2B and C represent salinity value

Fig. 3. Monthly variations of Σ REEs and SPM at different stations in Mandovi estuary.

Fig. 4. (A) Seasonal variations in the mean Σ REEs, SPM, salinity and $(L/H)_n$ at stations 1-7 in the Mandovi estuary (seasonal mean is obtained by averaging 4 analyses in 4 months). (B) PAAS-normalized REE patterns in SPM in the three seasons. Arrow in Post-monsoon (B) represents Shale (PAAS)-normalized REE patterns of Fe-Mn ORE.

Fig. 5. Spatial distributions of the mean Al, Fe and Mn (A-C), mean Ce and Eu anomalies (D-F) and, mean $(La/Yb)_n$, $(La/Gd)_n$, and $(Yb/Gd)_n$ (G-I) during monsoon, post-monsoon and pre-monsoon seasons in the SPM of Mandovi estuary. Ce and Eu anomalies were calculated using the equations, $Ce/Ce^* = 3Ce_{CN}/(2La_{CN} + Nd_{CN})$ and $Eu/Eu^* = Eu_{CN}/[Sm_{CN} \times Gd_{CN}]^{1/2}$ of Taylor and McLennan (1985). 'CN' denotes concentration normalized with respect to PAAS.

Fig. 6. Seasonal mean Σ REEs distributions (A) and the Shale (PAAS)-normalized REE patterns (B) in bottom sediments at different stations during the monsoon, post-monsoon and pre-monsoon. Arrow shows the samples from river-end (R) to sea-end (S) of the estuary.

Fig. 7. Relations for Σ REEs with Al, Fe and Mn in suspended and bottom sediment in different seasons in the Mandovi estuary.

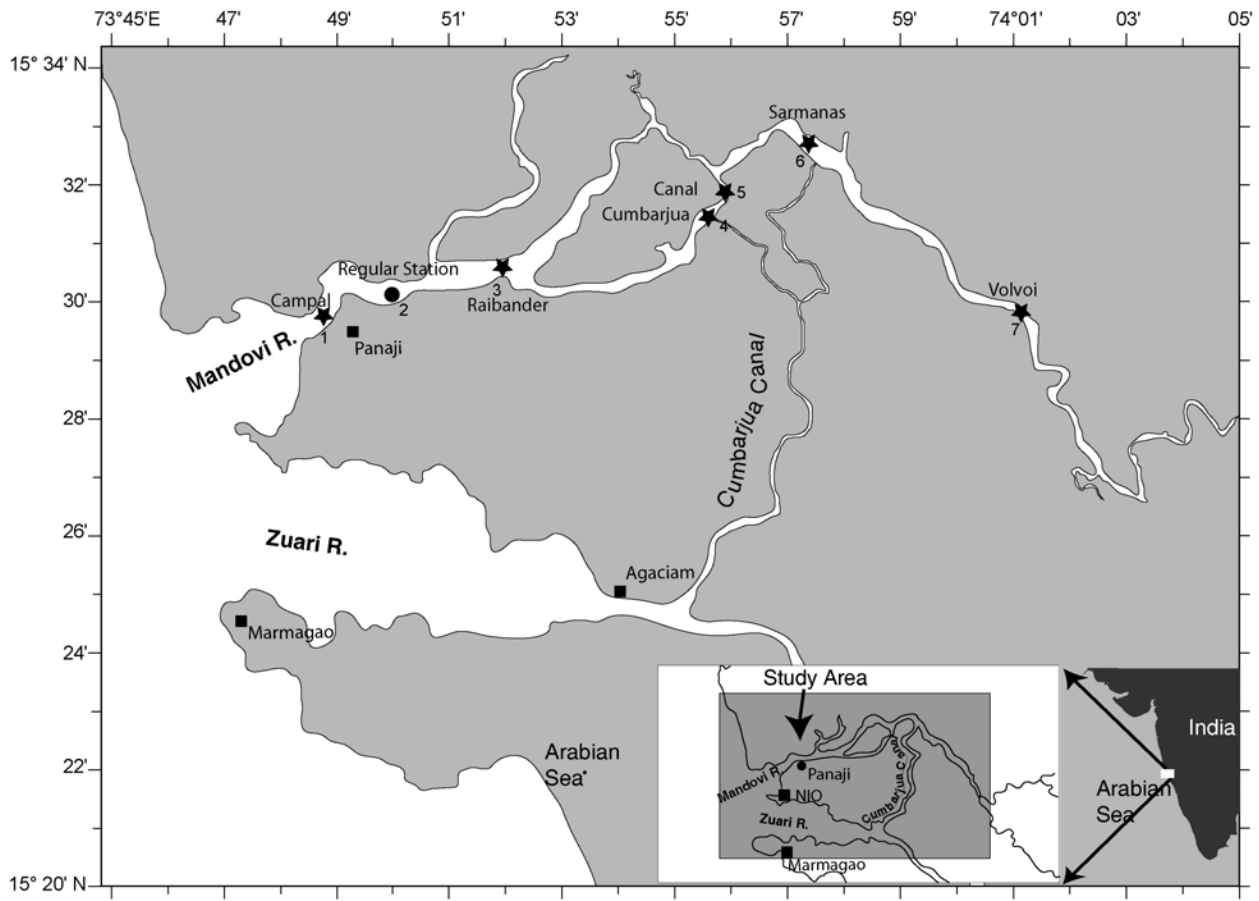


Fig. 1

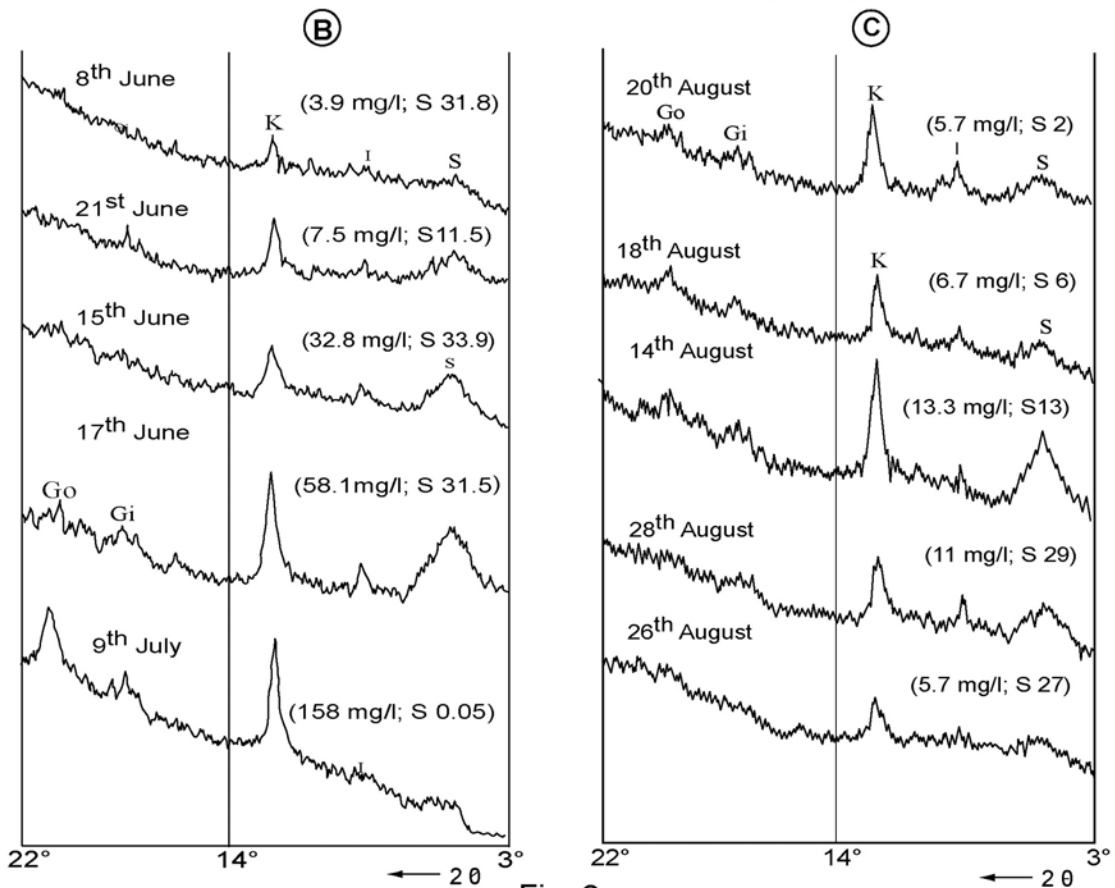
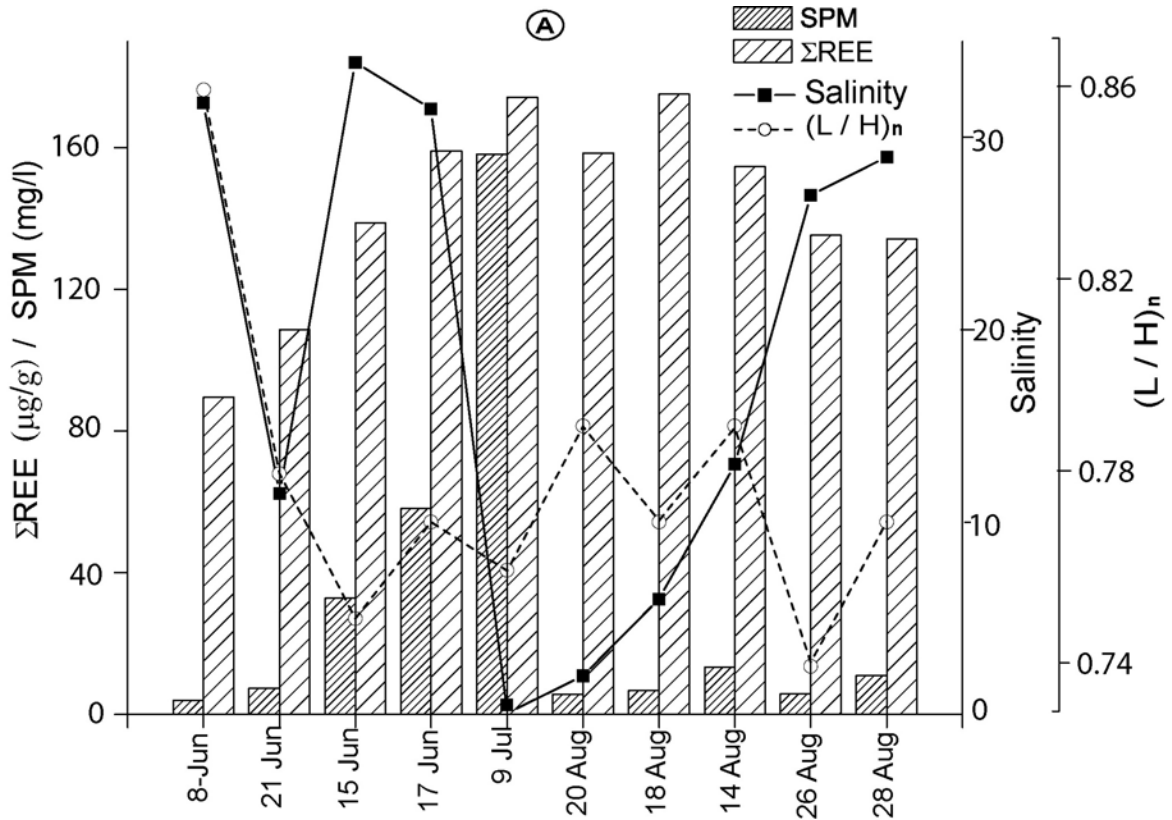


Fig. 2

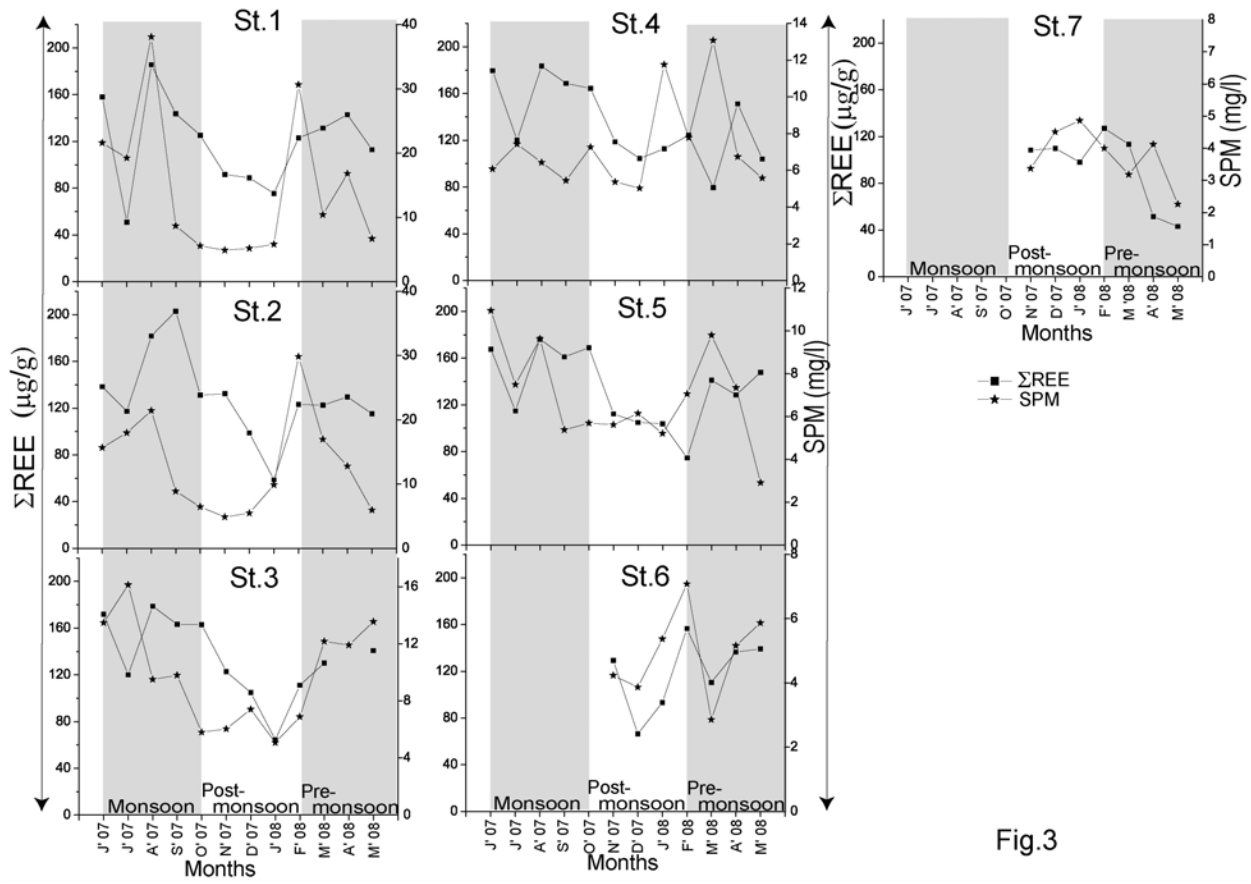


Fig.3

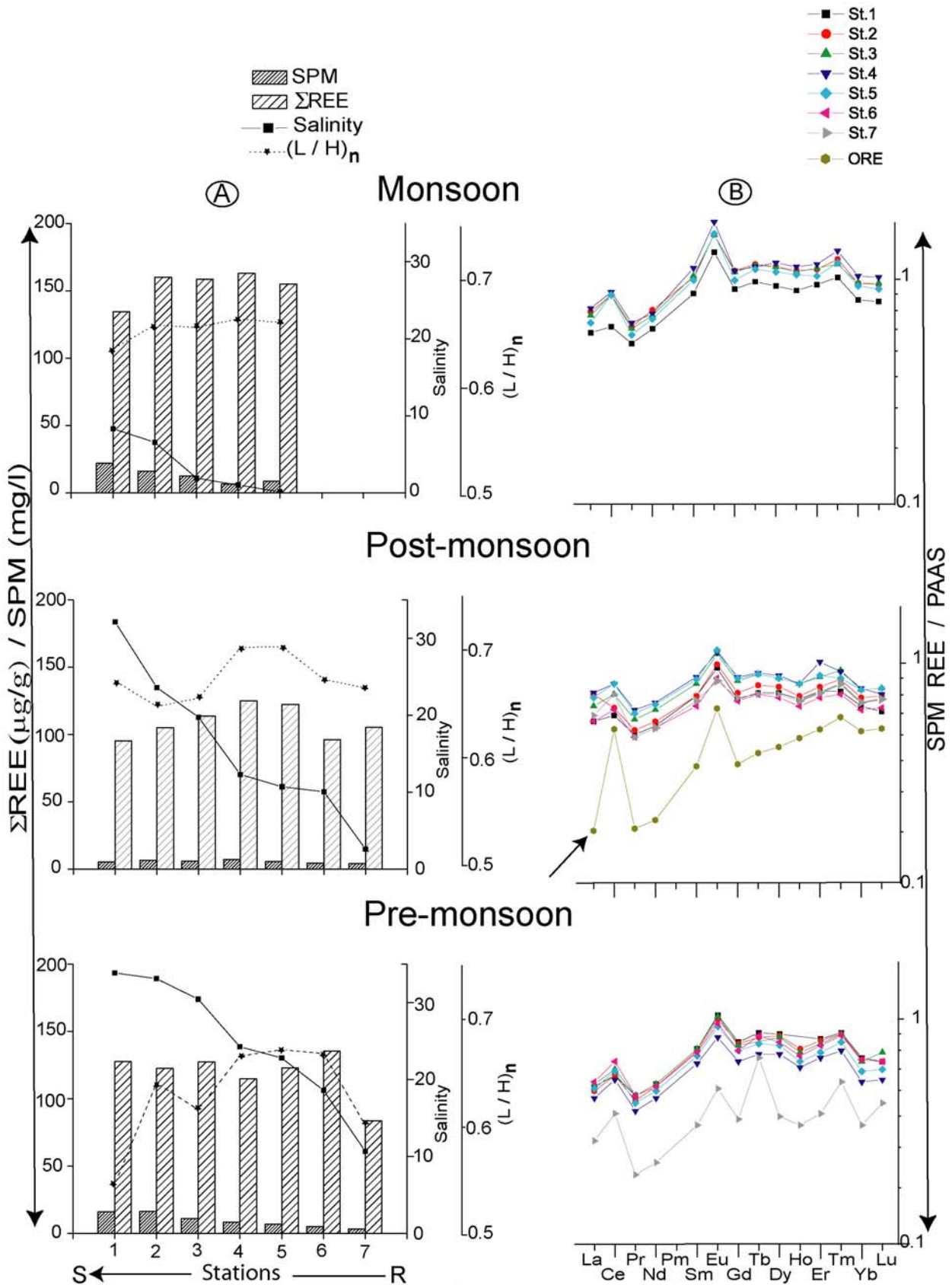


Fig.4

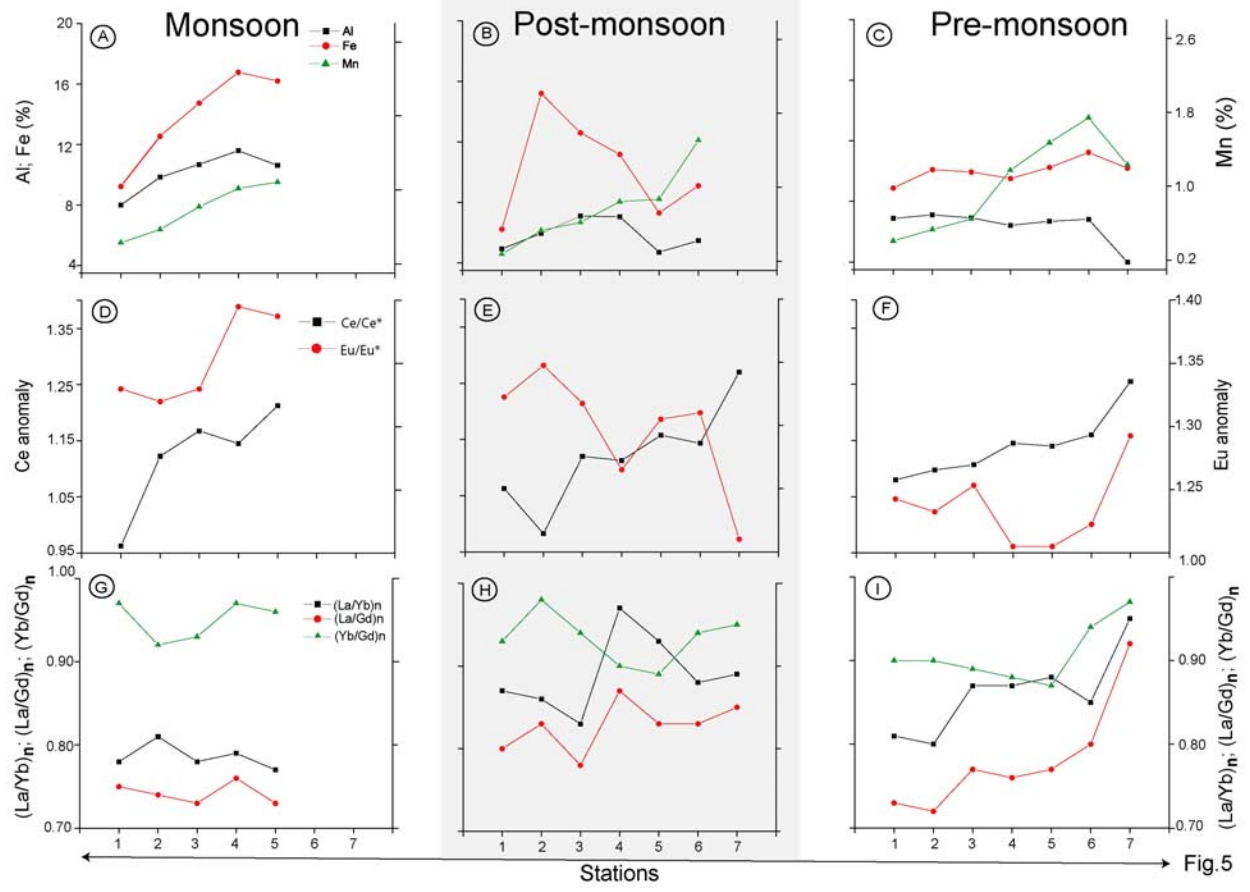


Fig.5

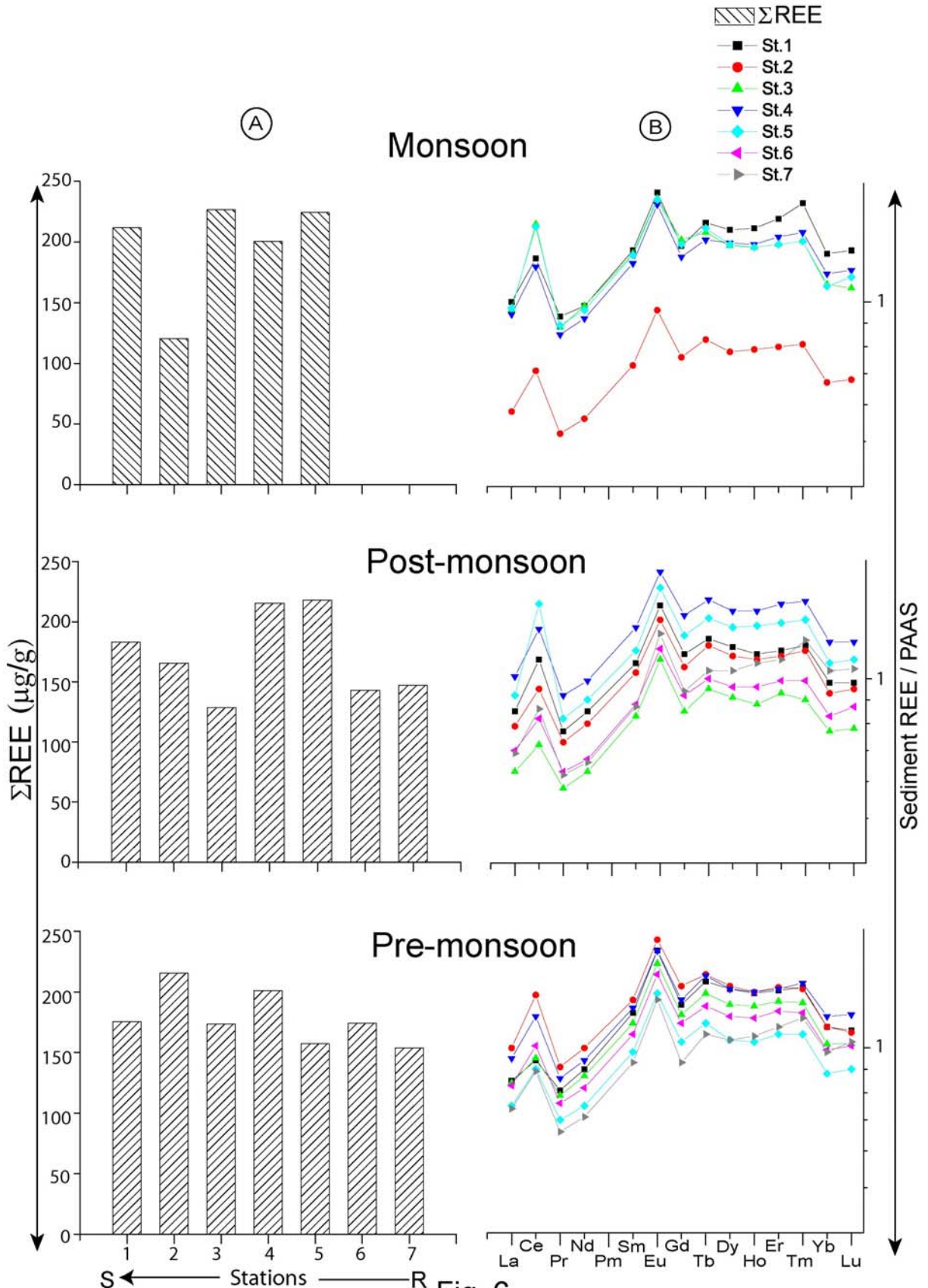


Fig. 6

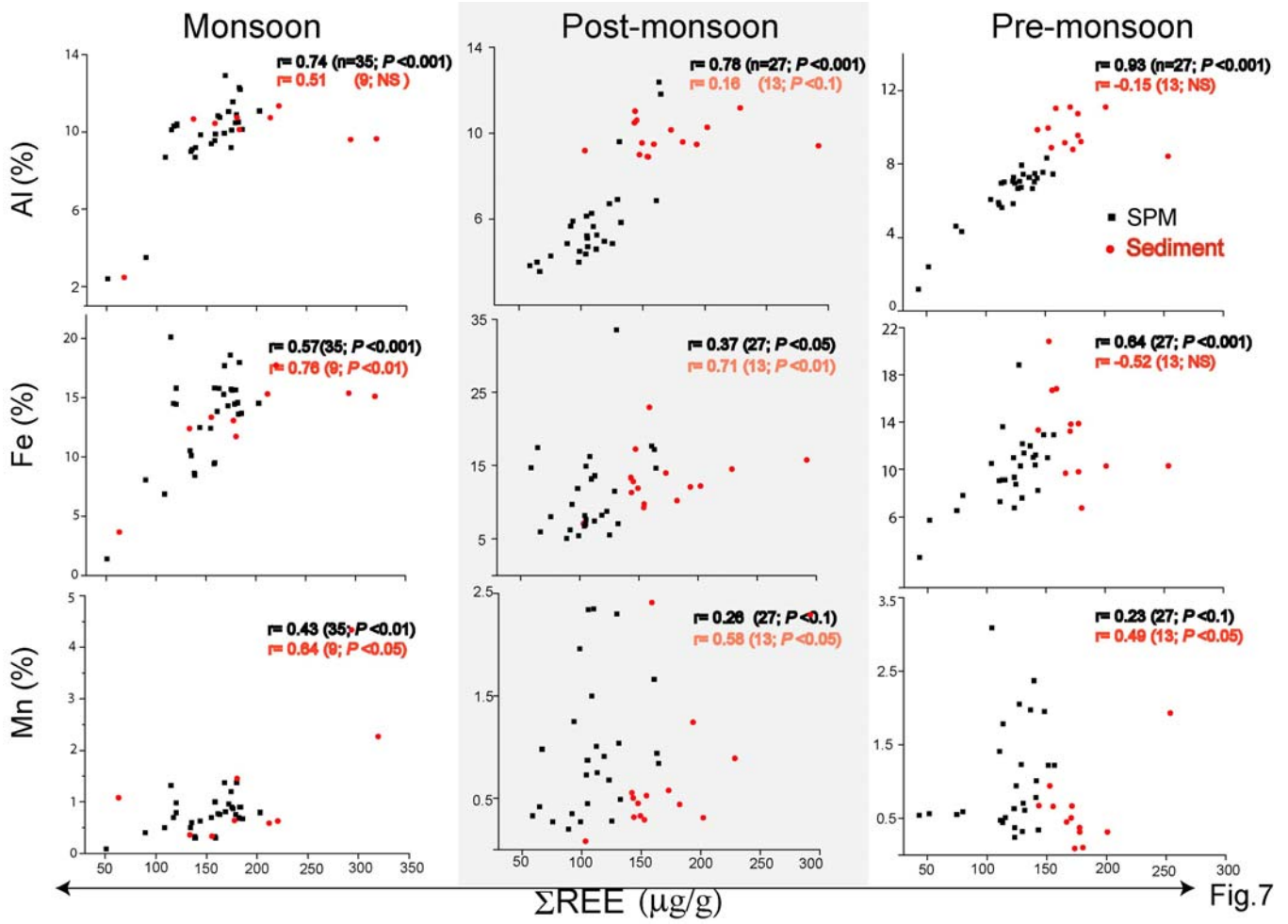


Fig.7

Table: 1
Analytical results of certified and obtained values of
USGS geochemical standard MAG-1 (All values in
ppm)

Elements	USGS Certified Values	This work Mean of 5 analysis
	Mean \pm SD	Mean \pm SD
Al (%)	8.66 \pm 0.16	8.20 \pm 0.18
Mn (%)	0.08 \pm 0.42	0.07 \pm 0.004
Fe (%)	4.58 \pm 0.0005	4.74 \pm 0.06
La	43 \pm 4	44.38 \pm 0.19
Ce	88 \pm 9	90.21 \pm 0.72
Pr	9.3	9.57 \pm 0.13
Nd	38 \pm 5	39.28 \pm 0.53
Sm	7.5 \pm 0.6	7.82 \pm 0.11
Eu	1.5 \pm 0.14	1.63 \pm 0.07
Gd	5.8 \pm 0.7	5.98 \pm 0.19
Tb	0.96 \pm 0.09	1.02 \pm 0.04
Dy	5.2 \pm 0.3	5.36 \pm 0.15
Ho	1.02 \pm 0.1	1.05 \pm 0.05
Er	3	3.15 \pm 0.08
Tm	0.43	0.46 \pm 0.01
Yb	2.6 \pm 0.3	2.65 \pm 0.04
Lu	0.4 \pm 0.04	0.42 \pm 0.02

Table 2
Major elements (%) and rare earth elements concentration ($\mu\text{g g}^{-1}$) in suspended particulate matter (SPM) at the regular station.

Dates	Al	Fe	Mn	Fe/Al	Mn/Al	La	Ce	Pr	Nd	Sm	Eu	Gd	Tb	Dy	Ho	Er	Tm	Yb	Lu	ΣREE	L/H^a	$(L/H)_n$	$(La/Yb)_n$	$(La/Gd)_n$	$(Yb/Gd)_n$	Eu/Eu*	Ce/Ce*
8-Jun	3.5	8.1	0.4	2.29	0.11	24.8	33.8	3.0	13.8	3.8	1.3	2.5	0.4	2.0	0.4	1.9	0.2	1.3	0.2	89.4	21.1	0.86	1.41	1.19	0.85	1.97	0.75
15-Jun	9.2	8.5	0.3	0.93	0.03	25.8	58.8	5.7	24.8	5.2	1.4	4.7	0.8	4.7	1.0	2.8	0.4	2.4	0.4	138.9	19.1	0.75	0.79	0.68	0.85	1.36	1.06
17-Jun	9.9	9.5	0.3	0.96	0.03	29.9	67.1	6.6	28.1	6.1	1.6	5.3	0.9	5.4	1.1	3.2	0.5	2.8	0.4	159.0	19.4	0.77	0.80	0.69	0.86	1.30	1.06
21-Jun	8.7	6.9	0.5	0.79	0.06	21.4	47.6	4.4	17.9	4.0	1.0	3.2	0.7	3.4	0.7	2.1	0.3	1.8	0.3	108.6	20.3	0.78	0.86	0.82	0.96	1.29	1.09
27-Jun	8.7	8.6	0.3	0.99	0.04	26.4	59.8	5.6	23.8	5.1	1.3	4.5	0.7	4.4	0.9	2.6	0.4	2.3	0.4	138.4	20.4	0.79	0.85	0.71	0.84	1.31	1.08
9-Jul	9.2	18.6	1.2	2.04	0.13	30.6	80.6	6.7	28.3	6.1	1.6	5.3	0.9	5.5	1.2	3.3	0.5	3.0	0.5	174.3	20.0	0.76	0.75	0.70	0.93	1.36	1.25
12-Jul	10.3	14.5	0.7	1.41	0.07	21.4	52.2	4.6	19.5	4.2	1.1	3.7	0.7	3.9	0.8	2.4	0.3	2.1	0.3	117.3	18.9	0.74	0.74	0.70	0.95	1.33	1.16
10-Aug	10.5	14.6	0.7	1.38	0.06	34.2	81.0	7.2	30.2	6.4	1.7	5.6	1.0	5.8	1.2	3.5	0.6	3.1	0.5	181.8	20.0	0.75	0.82	0.75	0.91	1.33	1.14
14-Aug	9.4	12.4	0.7	1.31	0.08	29.0	67.3	6.2	26.9	5.6	1.5	4.8	0.8	5.0	1.0	3.0	0.4	2.6	0.4	154.7	20.0	0.79	0.81	0.73	0.90	1.37	1.10
18-Aug	10.1	15.7	0.9	1.55	0.09	33.1	77.0	6.9	29.8	6.3	1.7	5.3	1.0	5.5	1.1	3.3	0.5	3.0	0.4	175.1	20.0	0.77	0.80	0.76	0.95	1.38	1.11
20-Aug	9.9	15.8	1.0	1.60	0.10	30.7	68.9	6.4	27.5	5.7	1.5	4.5	0.8	4.9	1.0	3.2	0.5	2.5	0.4	158.5	20.3	0.79	0.90	0.83	0.93	1.37	1.08
24-Aug	12.3	13.6	0.9	1.10	0.08	35.5	80.2	7.0	31.0	6.6	1.7	5.4	0.9	5.6	1.2	3.4	0.5	3.1	0.5	182.6	20.6	0.79	0.85	0.80	0.94	1.33	1.09
26-Aug	9.1	10.1	0.6	1.10	0.07	25.2	60.3	5.3	22.5	4.9	1.3	4.0	0.7	4.1	0.9	2.8	0.4	2.3	0.3	135.3	19.3	0.74	0.81	0.77	0.95	1.42	1.15
28-Aug	9.0	10.5	0.5	1.16	0.05	25.5	58.2	5.3	23.2	5.0	1.3	4.3	0.7	4.1	0.9	2.7	0.4	2.3	0.3	134.2	19.8	0.77	0.82	0.72	0.88	1.33	1.09
7-Sep	11.1	14.5	0.8	1.31	0.07	39.2	90.2	7.7	34.4	6.8	1.8	6.0	1.1	6.3	1.3	3.7	0.6	3.5	0.5	202.9	20.8	0.79	0.83	0.80	0.96	1.31	1.11
Mean	9.4	12.1	0.7	1.29	0.07	28.8	65.5	5.9	25	5.5	1.5	4.6	0.8	4.7	1.0	2.9	0.4	2.5	0.4	150.1	20.0	0.77	0.86	0.78	0.91	1.38	1.09
PAAS ^b	10.0	4.5	0.1	0.45	0.01	38.2	79.6	8.8	33.9	5.6	1.1	4.7	0.8	4.7	1.0	2.9	0.4	2.8	0.4	184.8	24.7						
ASSWR ^c	8.7	5.8	0.1	0.67	0.01	37.4	73.6	8.0	32.2	6.1	1.3	5.3	0.8	4.3	0.9	2.2	0.4	2.1	0.4	174.8	29.8						
UCC ^d	8.0	3.5	0.1	0.44	0.01	30.0	64.0	7.1	26.0	4.5	0.9	3.8	0.6	3.5	0.8	2.3	0.3	2.2	0.3	146.4	24.7						

^aL/H = LREE/HREE; LREE are La to Nd and HREE are Er to Lu (Rollinson, 1993); ^bPAAS - Post-Archaean average Australian shale (McLennan, 1989); ^cASSWR - Average suspended sediment in World Rivers (Viers et al., 2009); ^dUCC - Upper continental crust (Taylor and McLennan, 1985); Correlation of ΣREE with Al ($r=0.74$; $n=15$; $P<0.001$), Fe (0.67; 15; <0.01) and Mn (0.55; 15; <0.05) are discussed in the text.

Table 3

Mean concentration of major elements (%) and rare earth elements ($\mu\text{g g}^{-1}$) in suspended particulate matter (SPM) at the transect stations.

St.No	Al	Fe	Mn	Fe/Al	Mn/Al	La	Ce	Pr	Nd	Sm	Eu	Gd	Tb	Dy	Ho	Er	Tm	Yb	Lu	ΣREE	L/H	(L/H) _n	(La/Yb) _n	(La/Gd) _n	(Yb/Gd) _n	Ce/Ce*	Eu/Eu'
Monsoon																											
St.1	8.0	9.2	0.4	1.16	0.05	25.9	56.7	5.6	23.7	5.0	1.3	4.3	0.8	4.4	0.9	2.7	0.4	2.4	0.4	134.6	18.1	0.72	0.78	0.75	0.97	0.96	1.33
St.2	10.1	13.0	0.6	1.29	0.06	30.3	70.8	6.3	27.0	5.6	1.5	5.0	0.9	5.1	1.1	3.0	0.5	2.7	0.4	160.1	20.0	0.77	0.81	0.74	0.92	1.12	1.32
St.3	10.7	14.7	0.8	1.38	0.08	29.2	71.2	6.2	26.2	5.7	1.5	4.9	0.9	5.1	1.0	3.1	0.5	2.7	0.4	158.5	19.8	0.75	0.78	0.73	0.93	1.17	1.33
St.4	11.6	16.8	1.0	1.45	0.09	31.0	72.6	6.4	26.3	6.0	1.6	5.0	0.8	5.2	1.1	3.2	0.5	2.9	0.4	163.0	19.4	0.74	0.79	0.76	0.97	1.14	1.39
St.5	10.6	16.2	1.1	1.53	0.10	27.9	71.0	5.9	25.3	5.5	1.5	4.6	0.8	4.9	1.0	2.9	0.5	2.7	0.4	155.0	20.1	0.75	0.77	0.73	0.96	1.21	1.39
Mean	10.2	14.0	0.8	1.37	0.08	28.9	68.5	6.1	25.7	5.6	1.5	4.7	0.8	5.0	1.0	3.0	0.5	2.7	0.4	154.2	19.5	0.75	0.79	0.74	0.95	1.12	1.35
SD	1.34	3.03	0.27	2.26	0.20	2.02	6.61	0.34	1.26	0.36	0.11	0.27	0.04	0.31	0.06	0.17	0.03	0.17	0.03	11.37	0.83	0.02	0.02	0.01	0.03	0.10	0.04
Post-monsoon																											
St.1	4.9	6.2	0.3	1.26	0.06	18.9	41.4	3.8	15.9	3.5	0.9	2.9	0.5	3.0	0.6	1.9	0.3	1.6	0.2	95.3	19.9	0.78	0.87	0.80	0.93	1.06	1.32
St.2	6.0	15.2	0.5	2.55	0.09	24.3	44.3	4.0	16.5	3.5	0.9	3.0	0.5	3.2	0.6	2.0	0.3	1.8	0.3	105.2	20.7	0.75	0.86	0.83	0.98	0.98	1.35
St.3	7.1	12.6	0.6	1.78	0.09	21.8	51.0	4.4	18.7	4.0	1.0	3.4	0.6	3.5	0.7	2.2	0.3	1.9	0.3	113.7	20.0	0.76	0.83	0.78	0.94	1.12	1.32
St.4	7.1	11.2	0.8	1.58	0.12	24.9	56.4	4.9	20.0	4.2	1.0	3.5	0.6	3.6	0.7	2.5	0.3	1.9	0.3	125.0	21.7	0.85	0.97	0.87	0.90	1.11	1.27
St.5	4.7	7.3	0.9	1.55	0.19	23.9	56.3	4.7	19.6	4.1	1.1	3.5	0.6	3.5	0.7	2.2	0.3	1.9	0.3	122.5	22.2	0.85	0.93	0.83	0.89	1.16	1.30
St.6	5.5	9.1	1.5	1.66	0.28	18.6	44.0	3.7	15.5	3.2	0.8	2.8	0.5	2.9	0.6	1.8	0.3	1.6	0.2	96.4	21.3	0.81	0.88	0.83	0.94	1.14	1.31
St.7	5.3	13.8	1.9	2.59	0.36	20.0	50.9	3.7	15.7	3.3	0.8	2.9	0.5	3.0	0.6	1.8	0.3	1.7	0.3	105.5	22.3	0.80	0.89	0.85	0.95	1.27	1.21
Mean	5.8	10.8	0.9	1.86	0.16	21.8	49.2	4.2	17.4	3.7	0.9	3.1	0.5	3.3	0.6	2.0	0.3	1.8	0.3	109.1	21.2	0.8	0.9	0.8	0.9	1.1	1.3
SD	0.96	3.36	0.58	3.49	0.61	2.66	6.05	0.49	1.95	0.41	0.11	0.32	0.06	0.27	0.06	0.26	0.03	0.15	0.02	11.79	0.98	0.04	0.05	0.03	0.03	0.09	0.05
Pre-monsoon																											
St.1	6.9	8.9	0.4	1.29	0.06	23.6	53.7	5.1	21.5	4.5	1.1	3.9	0.7	4.2	3.8	2.5	0.4	2.1	0.3	127.6	19.6	0.77	0.81	0.73	0.90	1.08	1.24
St.2	7.0	9.3	0.5	1.32	0.06	23.1	53.3	5.0	21.0	4.4	1.1	3.9	0.7	4.2	3.8	2.4	0.4	2.1	0.3	122.6	19.5	0.76	0.80	0.72	0.90	1.10	1.23
St.3	6.9	9.9	0.6	1.44	0.09	24.2	56.0	5.1	21.4	4.5	1.1	3.9	1.0	4.1	3.8	2.4	0.4	2.1	0.3	127.4	20.7	0.78	0.87	0.77	0.89	1.11	1.25
St.4	6.4	9.5	1.2	1.48	0.18	21.6	51.5	4.6	19.2	4.0	0.9	3.4	0.6	3.6	3.7	2.2	0.3	1.8	0.3	114.8	21.1	0.80	0.87	0.76	0.88	1.15	1.20
St.5	6.7	10.2	1.5	1.53	0.22	23.3	55.3	4.9	20.4	4.3	1.0	3.7	0.6	3.9	3.7	2.3	0.3	2.0	0.3	123.0	21.5	0.81	0.88	0.77	0.87	1.14	1.20
St.6	6.8	11.2	1.7	1.65	0.26	25.7	61.8	5.3	22.2	4.6	1.1	3.9	0.7	4.2	3.8	2.5	0.4	2.2	0.3	135.6	21.5	0.80	0.85	0.80	0.94	1.16	1.22
St.7	4.0	10.2	1.2	2.56	0.31	16.1	40.5	2.9	12.1	2.6	0.7	2.3	0.6	2.3	3.5	1.4	0.3	1.3	0.2	83.7	22.1	0.74	0.95	0.92	0.97	1.25	1.29
Mean	6.39	9.90	1.02	1.55	0.16	22.5	53.2	4.69	19.7	4.12	1.00	3.57	0.71	3.79	1.16	2.23	0.34	1.95	0.31	119.3	20.8	0.78	0.86	0.78	0.91	1.14	1.24
SD	1.08	0.77	0.52	0.72	0.48	3.11	6.48	0.81	3.49	0.70	0.16	0.60	0.15	0.68	1.18	0.37	0.04	0.31	0.03	16.90	0.97	0.03	0.05	0.06	0.03	0.06	0.03

Table 4
Mean concentration of the major elements (%) and rare earth elements ($\mu\text{g g}^{-1}$) in surface sediments at the transect stations.

St.No	Al	Fe	Mn	Fe/Al	Mn/Al	La	Ce	Pr	Nd	Sm	Eu	Gd	Tb	Dy	Ho	Er	Tm	Yb	Lu	ΣREE	L/H	(L/H) _n	(La/Yb) _n	(La/Gd) _n	(Yb/Gd) _n	Ce/Ce*	Eu/Eu*
Monsoon																											
St.1	10.7	15.3	0.6	1.42	0.05	38.4	98.3	8.2	33.3	7.1	1.9	6.2	1.1	6.7	1.4	4.3	0.7	3.6	0.6	211.7	19.6	0.7	0.8	0.8	1.0	1.2	1.3
St.2	6.6	8.4	0.9	1.26	0.13	22.1	56.2	4.6	19.1	4.0	1.0	3.5	0.6	3.7	0.8	2.3	0.3	1.9	0.3	120.4	21.8	0.8	0.9	0.8	0.9	1.3	1.3
St.3	10.2	13.7	1.3	1.35	0.13	36.8	117.2	7.8	33.1	7.0	1.8	6.3	1.1	6.2	1.3	3.8	0.5	3.1	0.5	226.5	23.7	0.9	0.9	0.7	0.8	1.4	1.3
St.4	10.7	14.7	1.0	1.37	0.10	35.8	94.8	7.5	31.1	6.7	1.7	5.8	1.0	6.3	1.3	3.9	0.6	3.2	0.5	200.3	20.8	0.8	0.8	0.8	0.9	1.3	1.3
St.5	10.0	14.4	2.3	1.43	0.23	37.0	115.5	7.8	32.5	7.0	1.8	6.2	1.1	6.2	1.3	3.8	0.5	3.1	0.5	224.3	23.9	0.9	0.9	0.7	0.9	1.4	1.3
Mean	9.7	13.3	1.2	1.38	0.13	34.0	96.4	7.2	29.8	6.4	1.6	5.6	1.0	5.8	1.2	3.6	0.5	3.0	0.5	196.6	22.0	0.8	0.8	0.7	0.9	1.3	1.3
SD	1.73	2.81	0.67	1.63	0.39	6.71	24.61	1.48	6.07	1.32	0.34	1.17	0.21	1.21	0.25	0.78	0.12	0.64	0.10	43.90	1.85	0.06	0.04	0.02	0.05	0.10	0.02
Post-monsoon																											
St.1	9.8	13.0	0.9	1.33	0.09	32.6	87.8	6.8	28.7	6.0	1.6	5.3	0.9	5.5	1.1	3.3	0.5	2.8	0.4	183.2	22.5	0.8	0.9	0.8	0.9	1.3	1.3
St.2	9.6	11.1	0.4	1.16	0.04	30.1	75.8	6.4	27.1	5.7	1.5	5.0	0.9	5.2	1.1	3.2	0.5	2.6	0.4	165.6	20.8	0.8	0.8	0.7	0.9	1.2	1.3
St.3	9.1	8.4	0.3	0.93	0.03	23.9	57.2	5.1	21.5	4.6	1.2	4.0	0.7	4.3	0.9	2.6	0.4	2.2	0.3	128.7	19.4	0.8	0.8	0.7	0.9	1.1	1.3
St.4	10.7	13.4	0.6	1.25	0.06	38.7	101.8	8.1	33.7	7.1	1.8	6.4	1.1	6.5	1.4	4.1	0.6	3.4	0.5	215.4	21.1	0.8	0.8	0.7	0.9	1.3	1.3
St.5	10.2	13.6	1.3	1.33	0.13	35.1	115.0	7.2	30.4	6.4	1.7	5.8	1.0	6.0	1.3	3.8	0.5	3.0	0.5	217.8	23.3	0.8	0.8	0.8	0.9	1.5	1.3
St.6	10.5	13.3	0.5	1.27	0.05	26.6	65.7	5.5	22.9	4.9	1.2	4.3	0.8	4.5	1.0	2.8	0.4	2.3	0.4	143.2	20.3	0.8	0.8	0.8	0.9	1.2	1.3
St.7	9.0	17.2	0.5	1.91	0.05	26.5	68.4	5.5	22.5	4.8	1.3	4.4	0.8	4.9	1.1	3.1	0.5	2.9	0.5	147.2	17.6	0.7	0.7	0.7	1.1	1.3	1.4
Mean	9.9	11.9	0.7	1.21	0.07	32.1	87.5	6.7	28.3	6.0	1.5	5.3	1.0	5.5	1.1	3.4	0.5	2.8	0.4	182.1	21.4	0.8	0.8	0.7	0.9	1.3	1.3
SD	0.68	2.66	0.35	3.94	0.52	5.30	20.91	1.09	4.59	0.94	0.24	0.87	0.15	0.82	0.18	0.51	0.08	0.42	0.06	35.27	1.90	0.05	0.07	0.01	0.08	0.12	0.03
Pre-monsoon																											
St.1	9.2	8.5	0.2	0.93	0.02	32.4	74.6	7.2	30.5	6.6	1.7	5.8	1.1	6.3	1.3	3.8	0.5	3.1	0.5	175.4	18.3	0.7	0.8	0.7	0.9	1.1	1.3
St.2	9.6	12.1	1.2	1.26	0.12	38.1	103.3	8.1	33.9	7.1	1.9	6.3	1.1	6.4	1.3	3.8	0.5	3.1	0.5	215.4	22.9	0.9	0.9	0.7	0.8	1.3	1.3
St.3	9.2	8.2	0.3	0.89	0.03	32.1	75.8	7.0	29.5	6.3	1.6	5.5	1.0	5.8	1.2	3.6	0.5	2.9	0.4	173.3	19.6	0.8	0.8	0.7	0.9	1.1	1.3
St.4	11.1	10.3	0.3	0.93	0.03	36.5	93.5	7.6	31.9	6.8	1.8	5.9	1.1	6.3	1.3	3.8	0.6	3.3	0.5	200.8	20.7	0.8	0.8	0.8	0.9	1.2	1.3
St.5	10.5	13.6	0.7	1.29	0.06	28.7	72.0	6.2	25.5	5.4	1.4	4.8	0.9	4.9	1.0	3.1	0.4	2.5	0.4	157.2	20.9	0.8	0.9	0.7	0.9	1.2	1.3
St.6	10.9	15.0	0.6	1.38	0.06	31.8	80.4	6.7	27.8	5.9	1.6	5.3	0.9	5.5	1.1	3.4	0.5	2.8	0.4	174.1	20.6	0.7	0.8	0.7	0.9	1.2	1.3
St.7	9.4	18.8	0.8	1.99	0.08	28.3	71.1	5.8	24.1	5.2	1.4	4.3	0.8	4.9	1.1	3.2	0.5	2.8	0.4	153.8	18.9	0.6	0.8	0.8	1.1	1.2	1.4
Mean	9.9	10.5	0.5	1.06	0.05	33.5	83.9	7.2	30.3	6.4	1.7	5.7	1.0	5.9	1.2	3.6	0.5	3.0	0.5	184.4	20.5	0.8	0.8	0.7	0.9	1.2	1.3
SD	0.82	3.78	0.34	4.59	0.41	3.63	12.25	0.78	3.47	0.70	0.18	0.69	0.11	0.65	0.12	0.32	0.05	0.28	0.04	22.28	1.50	0.08	0.05	0.04	0.08	0.07	0.02